Development/Plasticity/Repair

Emx2 and *Pax6* Function in Cooperation with *Otx2* and *Otx1* to Develop Caudal Forebrain Primordium That Includes Future Archipallium

Jun Kimura,[1]* Yoko Suda,[1]* Daisuke Kurokawa,[1] Zakir M. Hossain,[1] Miwa Nakamura,[1] Maiko Takahashi,[1] Akemi Hara,[2] and Shinichi Aizawa[1]

Laboratories for [1]Vertebrate Body Plan and [2]Animal Resources and Genetic Engineering, Center for Developmental Biology, RIKEN Kobe, Chuo-ku, Kobe 650-0047, Japan

One of the central issues in developmental neurobiology is how the forebrain is organized ontogenetically. The traditional view is that the anterior neuroectoderm first develops into mesencephalic and prosencephalic vesicles; the latter vesicle subsequently develops into the diencephalon and secondary prosencephalon, of which dorsal parts protrude to generate the telencephalon. The diencephalon yields the pretectum, thalamus, and prethalamus, and the telencephalon produces the archipallium, neopallium, and ganglionic eminences. By identifying cell descendants that once expressed *Emx2* with use of the *Cre* knock-in mutant into the *Emx2* locus and analyzing phenotypes of double mutants between *Emx2* and *Otx2/Otx1* and between *Emx2* and *Pax6*, we propose that at the 3–6 somite stage, the anterior neuroectoderm develops into three primordia: midbrain, caudal forebrain, and rostral forebrain. The caudal forebrain primordium generates not only the pretectum, thalamus, and prethalamus but also the archipallium, cortical hem, choroid plexus, choroidal roof, and eminentia thalami. The primordium corresponds to the *Emx2*- or *Pax6*-positive region at the 3–6 somite stage that most probably does not include the future neopallium or commissural plate. *Otx2* and *Otx1* that are expressed in the entire future forebrain and midbrain cooperate with this *Emx2* and *Pax6* expression in the development of the caudal forebrain primordium; *Emx2* and *Pax6* functions are redundant. In the embryonic day 9.5 $Emx2^{-/-}Pax6^{-/-}$ double mutant, the caudal forebrain remained unspecified and subsequently transformed into tectum in a mirror image of the endogenous one.

Key words: Emx2; *Pax6*; *Otx2*; forebrain; archipallium; diencephalon; tectum

Introduction

The rostral brain comprises a series of structures rostrocaudally and dorsoventrally. It is widely accepted that in front of the midbrain, the forebrain consists caudorostrally of the pretectum (p1), thalamus (dorsal thalamus, p2) and prethalamus (ventral thalamus, p3) (Puelles and Rubenstein, 1993, 2003). However, it is still a matter of dispute how forebrain structures in front of the prethalamus are organized; moreover, it is not yet certain how the forebrain is regionalized into these structures ontogenetically. An initial version of the prosomeric model postulated the archipallium and eminentia thalami as p4 structures rostral to p3 prethalamus and caudal to p5 neopallium (here "caudal forebrain" is used to indicate these p1 to p4 structures). In the traditional view, however, the archipallium is a dorsomedial structure, the neopallium is a dorsolateral structure, and ganglionic eminences are ventral structures of the telencephalon rostrally to the prethalamus (here "telencephalon" is used in this sense).

The initial morphological landmark in the anterior neuroectoderm is the preotic sulcus. In the neural plate rostral to this sulcus, a series of transcriptional factors, *Otx2*, *Gbx2*, *Pax2*, *En1*, *Pax6*, *Irx3*, and *Six3*, are expressed in a nested pattern, initially partly overlapping each other but being distinctly segregated by the 6–8 somite stage. This, together with the overexpression/ectopic expression studies in avian, led to a proposal that mutually inhibitory interactions among these genes determine the boundaries between each territory in the rostral brain (Kobayashi et al., 2002). The view proposes three divisions in the initial brain regionalization: forebrain rostral to zona limitans intrathalamica (ZLI), that caudal to ZLI, and midbrain. Another view in avian proposes that in the forebrain, the pretectum first differentiates and the thalamus and prethalamus are formed with the ZLI development (Larsen et al., 2001). Several mouse mutants are reported that exhibit defects in rostral brain development: *Pax2/5*, *En2/En1*, *Pax6* (*Sey*), *Six3*, and *Hesx1* (Stoykova et al., 1996; War-

Received Jan. 18, 2005; revised April 3, 2005; accepted April 3, 2005.

This work was supported by a grant-in-aid for Scientific Research on Priority Areas from the Ministry of Education, Culture, Sports, Science and Technology of Japan. We thank Dr. Luis Puelles for critical reading of this manuscript and Dr. S. Yonemura and N. Inoue for semithin and ultrathin analyses. We are indebted to Drs. K. Abe, A. P. McMahon, J. L. R. Rubenstein, P. Gruss, D. J. Anderson, P. Charnay, M. Taira, M. Frohman, H. Clevers, A. Joyner, D. G. Wilkinson, G. Martin, E. Lai, T. Miyamoto, and T. Ogura for providing *in situ* hybridization probes and to Drs. H. Hamada, V. van Heyningen, and N. Osumi and The Jackson Laboratory for providing *Lefty-Cre*, *Sey*, and ROSA26R mice. We are grateful to the Laboratory for Animal Resources and Genetic Engineering for the generation of the $Emx2^{+/Cre}$ mutant and for the housing of mice.

*J.K. and Y.S. contributed equally to this work.

Correspondence should be addressed to Dr. Shinichi Aizawa, Laboratory for Vertebrate Body Plan, Center for Developmental Biology, RIKEN Kobe, 2-2-3 Minatojima Minami-machi, Chuo-ku, Kobe 650-0047, Japan. E-mail: saizawa@cdb.riken.go.jp.

DOI:10.1523/JNEUROSCI.0239-05.2005

 0270-6474/05/255097-12$15.00/0

ren and Price, 1997; Schwarz et al., 1999; Martinez-Barbera et al., 2000; Liu and Joyner, 2001; Lagutin et al., 2003). However, the details of the defects, their processes, and the primary limits remain for future studies to synthesize ontogeny of forebrain structures.

Previously, we reported that in the $Emx2^{-/-}Otx2^{+/-}$ mutant, the commissure region of the pretectum develops but the non-commissure region of the pretectum, prethalamus, and thalamus are lost (Suda et al., 2001). In contrast, the ectopic *Emx2* expression over the entire forebrain and midbrain in the *Otx2* locus ($Otx2^{+/Emx2}$) is specifically incompatible with the development of the commissure region of the pretectum. *Emx2* is not expressed in the pretectum or thalamus when they are formed. Moreover, the *Otx2* expression is not unique to the caudal forebrain; How is the caudal forebrain specified in the $Emx2^{-/-}$ mutant? This situation can be explained simply by postulating a third gene, *X*, the expression of which overlaps and is functionally redundant with the *Emx2* expression. Here, we propose that *X* is the *Pax6* gene and that the caudal forebrain primordium spanning from the future pretectum to the archipallium is established against rostral forebrain and midbrain primordia at the 3–6 somite stage through the cooperation of *Emx2* and *Pax6* with *Otx*2 and *Otx1*.

Materials and Methods

Mutant mice. Emx2, *Emx1* (Yoshida et al., 1997), *Otx2* (Matsuo et al., 1995), and *Otx1* (Suda et al., 1997) mutant mice were generated as described. The sources of *Sey* and ROSA26R mice are as described previously (Hill et al., 1991; Soriano, 1999). Mice were housed in environmentally controlled rooms under the institute guidelines for animal and recombinant DNA experiments.

Generation of Cre knock-in mutant into Emx2 locus. To construct the targeting vector, the neomycin-resistant gene directed by the *PGK* gene promoter and polyadenylation (polyA) signal (neo) was flanked with *loxP* sequences; moreover, this was conjugated to the Cre recombinase gene (*Cre*) that lacks the polyA signal, generating the *Cre-neo* cassette. A DNA fragment encompassing 6.8 kb 5′ upstream to 2.3 kb 3′ downstream of the translation initiation site of the *Emx2* gene was isolated from C57BL/6 genomic DNAs. The *Cre-neo* cassette was inserted into the translational initiation codon of this fragment; ATG of the *Cre* gene corresponds to ATG of the *Emx2* gene (supplemental Fig. 2, available at www.jneurosci.org as supplemental material). The diphtheria toxin-A fragment gene, driven by the MC1 promoter, was used for negative selection of homologous recombinants as described previously (Yagi et al., 1993b). Details of the vector construction will be provided on request. The vector was linearized with *Not*I digestion, homologous recombinants were isolated with TT2 embryonic stem cells, and mutant mice ($Emx2^{+/Cre\text{-}neo}$) were generated as described previously (Yagi et al., 1993a). The mice were mated with *Lefty-Cre* mice (Yamamoto et al., 2001) to excise neo, generating $Emx2^{+/Cre}$ mice.

Genotyping of mice. Genotypes of mice and embryos were determined routinely by PCR; genomic DNAs were obtained from tails or yolk sacs. The primers used to identify *Emx2*, *Emx1*, *Otx2*, *Otx1*, *Pax6*, and ROSA26R wild-type and mutant alleles were as described previously (Grindley et al., 1995; Matsuo et al., 1995; Suda et al., 1997; Yoshida et al., 1997; Soriano, 1999). Those primers used to detect the *Cre-neo* knock-in allele in the *Emx2* locus were the 5′ primer (5′-GCCTGCTTGCCGAATATCATGGTGGAAAAT-3′) in the *neo* gene and the 3′ primer (5′-GACTGGAATTGGCGTAGCTGAGTG-3′) in the first exon of the *Emx2* gene; the primers used to detect the *Cre* knock-in allele were the 5′ primer (5′-AAGAAGCGAACACTTCCATGGATTGTC-3′) in the 5′ untranslated region of the *Emx2* gene and the 3′ primer (5′-CGAACATCTTCAGGTTCTGCGG-3′) in the *Cre* gene.

Histochemical analysis. β-Galactosidase (βGal) staining and histolog-

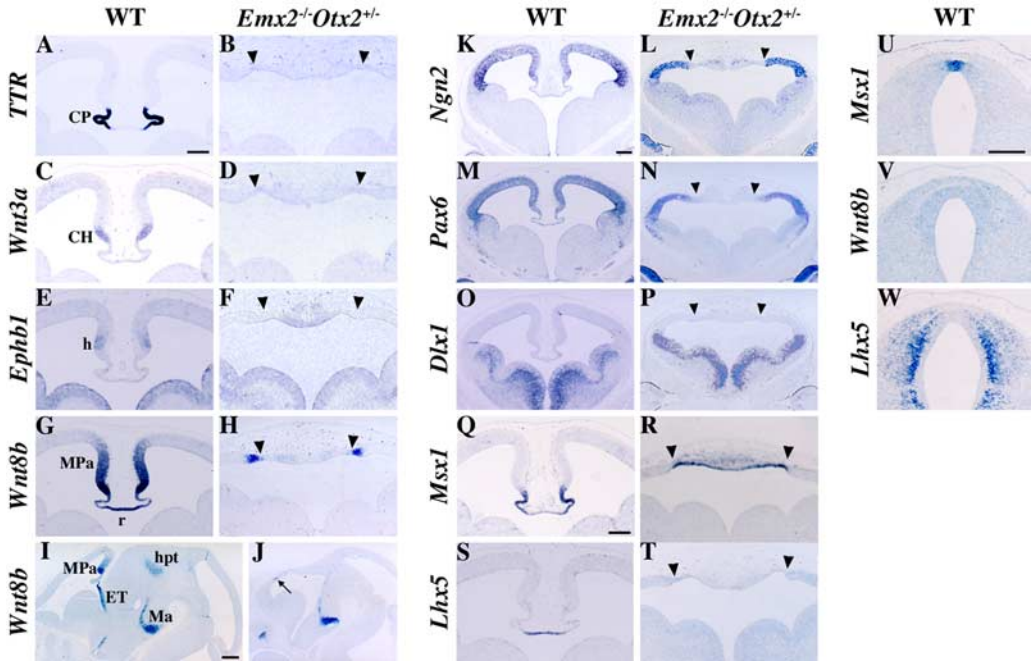

Figure 1. Marker analysis of archipallial defects in the E12.5 $Emx2^{-/-}Otx2^{+/-}$ mutant. The images give sagittal (***I***, ***J***) and frontal views at the telencephalic (***A–H***, ***K–T***) and mesencephalic (***U–W***) levels; the markers and genotypes of embryos examined are indicated to the left and at the top, respectively. In wild-type embryos (WT), *TTR* demarcates the choroid plexus (CP; ***A***), *Wnt3a* demarcates the cortical hem (CH; ***C***), and *Ephb1* demarcates the prospective hippocampus (h; ***E***). They are absent in the double mutant (***B***, ***D***, ***F***). Normally, *Wnt8b* is expressed in the medial pallium (MPa; ***G***, ***I***), eminentia thalami (ET; ***I***), vicinity of habenulopeduncular tract (hpt; ***I***), and mammillary region (Ma; ***I***). In the double mutant, the *Wnt8b*-positive mammillary region is present (***J***) but the medial pallium is residual (***H***, arrow in ***J***); *Wnt8b*-positive eminentia thalami and habenulopeduncular tract vicinity are lost (***H***, ***J***). The *Ngn2*- and *Pax6*-positive neopallium (***K***, ***M***) is present laterally in the double mutant (***L***, ***N***); the *Dlx1*-positive subpallium is normally found (***O***, ***P***). In this stage of the wild-type telencephalon, the *Msx1* expression is intense in the choroid plexus and ventral cortical hem but weak in the choroidal roof (***Q***); the *Msx1* expression is intense in the double mutant roof (***R***). The wild-type choroidal roof (r) expresses *Wnt8b* (***G***) and *Lhx5* (***S***), whereas the double mutant roof does not express either of them (***H***, ***T***). Of note is that the midbrain roof expresses *Msx1* intensively (***U***) but not *Wnt8b* (***V***) or *Lhx5* (***W***). Arrowheads in the double mutant panels indicate the medial limits of the *Wnt8b*-positive medial pallium that correspond to the lateral limits of the *Msx1*-positive roof. Scale bars, 240 μm.

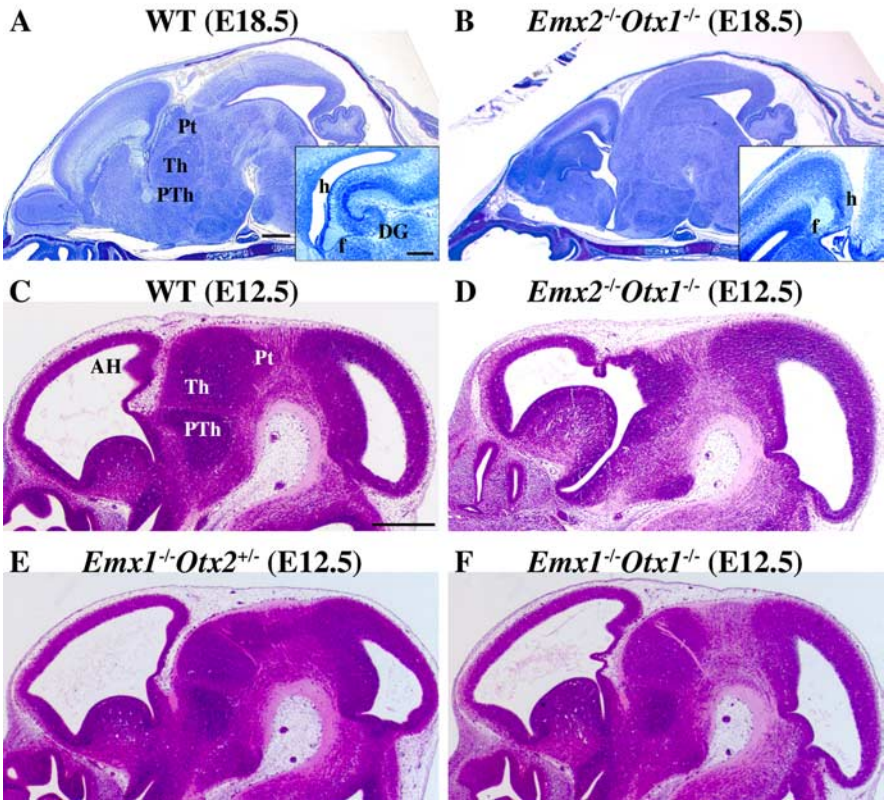

Figure 2. *Emx2/Otx1*, *Emx1/Otx2*, and *Emx1/Otx1* double mutant phenotypes. Sagittal sections of E18.5 embryos stained with cresyl violet (***A***, ***B***) and E12.5 embryos stained with hematoxylin and eosin (***C–F***) are shown. The insets in ***A*** and ***B*** show enlarged views of the hippocampal region. The *Emx2/Otx1* double mutant exhibits forebrain defects similar to but milder than the *Emx2/Otx2* double mutants (***B***, ***D***). Defects were not apparent in either the *Emx1/Otx2* (***E***) or the *Emx1/Otx1* (***F***) double mutant. AH, Ammon's horn; DG, dentate gyrus; f, fimbria; h, hippocampus; Pt, pretectum; PTh, prethalamus; Th, thalamus. Scale bars: ***A***, ***C***, 500 μm; ***A***, inset, 250 μm.

ical analysis were performed as described previously (Suda et al., 2001; Kurokawa et al., 2004a).

RNA in situ *hybridization.* Section and whole-mount *in situ* hybridization were performed using digoxigenin probes as described previously (Wilkinson, 1993). The probes used were as follows: *BF1* (Tao and Lai, 1992), *Dlx1* (Bulfone et al., 1993), *Dmbx1* (Miyamoto et al., 2002), *Ebf1* (Garel et al., 1997), *Emx2* and *Emx1* (Yoshida et al., 1997), *En2* (Davis and Joyner, 1988), *EphrinA2* (Flenniken et al., 1996), *Ephb1* (IMAGE clone AA058194), *Fgf8* (Crossley et al., 1996), *Gbx2* (Bulfone et al., 1993), *Irx1* (Bosse et al., 1997), *Lhx2* (Porter et al., 1997), *Lhx5* (Sheng et al., 1997), *Lim1* (Fujii et al., 1994), *Msx1* (Hill et al., 1989), *Ngn2* (Sommer et al., 1996), *Otx2* (Matsuo et al., 1995), *Pax2* (Dressler et al., 1990), *Pax6* (Stoykova et al., 1996), *Shh* (Echelard et al., 1993), *Six3* (Oliver et al., 1995), *Tcf4* (Korinek et al., 1998), *TTR* (Wakasugi et al., 1985), *Wnt3a* (Roelink and Nusse, 1991), *Wnt7b* (Parr et al., 1993), and *Wnt8b* (IMAGE clone AA170920).

Results

Archipallium, choroid plexus, and eminentia thalami are also lost in *Emx2*$^{-/-}$*Otx2*$^{+/-}$ double mutant

Our previous study demonstrated that the prethalamus, thalamus, and anterior pretectum are lost in the *Emx2*$^{-/-}$*Otx2*$^{+/-}$ double mutant; however, the analysis was incomplete as to the defects in more anterior regions (Suda et al., 2001). The double mutant does not develop beyond embryonic day 15.5 (E15.5) (Suda et al., 2001). In this telencephalon, the neopallium was reduced with a disorganized laminar structure; the cortical plate was hardly visible. Ganglionic eminences were hyperplastic. However, these regions were present whereas neither the CA fields, dentate gyrus, fimbria, nor choroid plexus was formed at E15.5, and Ammon's horn was not apparent at E12.5. To confirm this telencephalic phenotype, analyses were made with molecular markers. In the most medial pallium adjacent to the roof, transthiretin (*TTR*)-positive choroid plexus develops (Fig. 1*A*); it is adjacent to the *Wnt3a*-, *Wnt5a*-, and *Wnt2b*-positive fimbria or cortical hem (Fig. 1*C*) (Grove et al., 1998). *Ephb1* and *Prox1* expressions cover the hippocampal field (Fig. 1*E*) (data not shown), and *Wnt8b* and *Lef1* expressions cover the entire medial pallium (Fig. 1*G*,*I*) (data not shown). Neither the *TTR*-, *Wnt3a*-, *Wnt5a*-, *Wnt2b*-, *Ephb1*-, nor *Prox1*-positive structure was apparent in the *Emx2/Otx2* double mutant (Fig. 1*B*,*D*,*F*) (data not shown). The *Wnt8b* and *Lef1* expression was residual in the medial pallium (Fig. 1*H*) (data not shown), and *Wnt8b*-positive eminentia thalami were lost (Fig. 1*J*). In contrast, the *Wnt8b*-negative and *Ngn2*- and *Pax6*-positive neopallium developed laterally; the *Dlx1*-positive subpallium was formed almost normally (Fig. 1*L*,*N*,*P*).

Morphologically, the midline structure between *Wnt8b*-positive remnants in the double mutant (the structure between two arrowheads in Fig. 1) was the roof; however, it was not the telencephalic roof. In the wild-type dorsal telencephalon, *Msx1* is intense in the choroid plexus and ventral cortical hem and weak in the roof (Fig. 1*Q*). The *Msx1* expression was intense in the double mutant roof (Fig. 1*R*). The wild-type choroidal roof expresses *Wnt8b* (Fig. 1*G*) and *Lhx5* (Fig. 1*S*); the double mutant roof expressed neither of them (Fig. 1*H*,*T*). The midbrain roof expresses *Msx1* intensively (Fig. 1*U*), whereas it does not express *Wnt8b* (Fig. 1*V*) or *Lhx5* (Fig. 1*W*).

Thus, we conclude that in the *Emx2*$^{-/-}$*Otx2*$^{+/-}$ double mutant, in addition to the prethalamus, thalamus, and anterior pretectum we described previously (Suda et al., 2001), the archipallium, cortical hem, choroid plexus, choroidal roof, and eminentia thalami fail to develop. The rostral forebrain territory of ganglionic eminences, neopallium, and the *Fgf8*-positive commissural plate, however, develop. A question remains as to the lateral/dorsal limit of the medial pallium loss in the double mutant. As discussed below, the intensity of the *Emx2* expression is discontinuous at a boundary between the archipallium and neopallium (see Fig. 3*Bb*). The limit of the medial pallium defect probably corresponds to this boundary. Histologically, hippocampal structures were entirely absent at E15.5 (Suda et al., 2001), and *Ephb1*- and *Prox1*-positive regions were completely missing. We speculate that the *Wn8b* and *Lef1* expressions extend into the most medial neopallium or the cingulate/retrosplenial neopallium (Shinozaki et al., 2004); the residual *Wnt8b*- and *Lef1*-positive regions in the double mutant may represent this most medial neopallium. However, no data exist that demonstrates the structures to which the dorsalmost/lateralmost aspect of the *Wnt8b*- and *Lef1*-positive regions actually correspond.

Otx1 cooperates with *Emx2*, but *Emx1* does not cooperate with *Otx2* or *Otx1*, in forebrain development

Otx2 and *Emx2* have cognates, *Otx1* and *Emx1*, respectively. It was then examined whether these cognates also participate in forebrain development. Histologically, development of the prethalamus, thalamus, and pretectum was meager in the E18.5 and E12.5 $Emx2^{-/-}Otx1^{-/-}$ double mutant (Fig. 2*B*,*D*). The telencephalon was smaller, but the choroid plexus developed in the double mutant. The hippocampal field developed poorly at E18.5 (Fig. 2*B*, inset), and at E12.5, Ammon's horn was markedly deformed (Fig. 2*D*). Molecular marker analyses at E12.5 with *Ebf1*, *Lim1*, *Gbx2*, *Tcf4*, *Pax6*, and *Dlx1* indicated that only abnormal remnants of the anterior pretectum, thalamus, and prethalamus remained in the $Emx2^{-/-}Otx1^{-/-}$ mutant (supplemental Fig. 1, available at www.jneurosci.org as supplemental material). The analyses on *Ephb1*, *Lef1*, and *Wnt8b* expression also suggested great reduction in the medial pallium (data not shown). Thus, *Emx2* cooperates not only with *Otx2* but also with *Otx1* for forebrain development. In contrast, defects were not apparent in the forebrain of either the $Emx1^{-/-}Otx2^{+/-}$ or the $Emx1^{-/-}Otx1^{-/-}$ mutant (Fig. 2*E*,*F*); *Emx1* does not cooperate with *Otx2* or *Otx1*. This is consistent with the later onset of *Emx1* expression at approximately E9.5 (Simeone et al., 1992; Yoshida et al., 1997) in a more limited region of the forebrain, the pallium.

Origin of the thalamus and pretectum cells

The *Emx2* mRNA expression is not found at E9.5 in the region posterior to ZLI (Fig. 3*Ac*) (Simeone et al., 1992; Suda et al., 2001). At E12.5, the expression is persistent in the pallium, whereas it is faint in eminentia thalami and others (Fig. 3*Ad*). Obviously, the *Emx2* expression narrows with the forebrain development. To determine cell descendants that once expressed *Emx2*, mice were generated in which the Cre recombinase gene was knocked-in into the *Emx2* locus (supplemental Fig. 2, available at www.jneurosci.org as supplemental material) and mated with ROSA26R mice (Soriano, 1999). The analysis has inherent problems of incomplete and ectopic Cre-mediated recombination, but the βGal expression in embryos that harbor both *Cre* in the *Emx2* locus and ROSA26R clearly demonstrated the cells that once expressed *Emx2*. At E9.5, the βGal-positive region was found in the intermediate mesoderm, eyes, nose, and

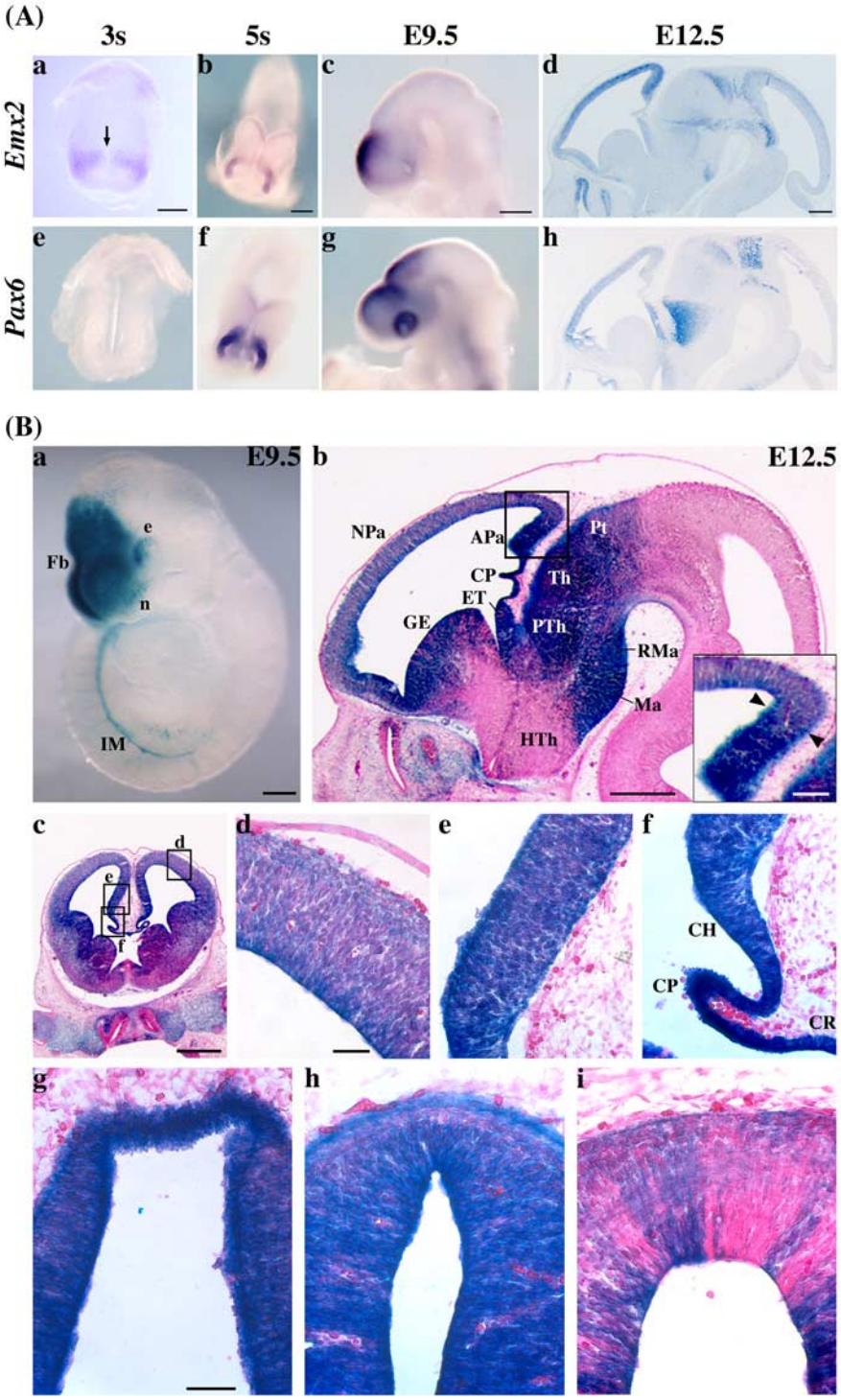

Figure 3. Analysis of cell descendants that once expressed *Emx2*. ***A***, *Emx2* and *Pax6* mRNA expression at stages indicated at the top. Anterior is at the bottom (***a***, ***b***, ***e***, ***f***) and to the left (***c***, ***d***, ***g***, ***h***). The arrow in ***a*** indicates the absence of the *Emx2* expression in the midline or future ventral diencephalon. s, Somite stage. Scale bars: (in ***a***, ***b)*** ***a***, ***b***, ***e***, ***f***, 125 μm; (in ***c***, ***d***) ***c***, ***d***, ***g***, ***h***, 250 μm. ***B***, βGal expression in ROSA26R/$Emx2^{+/Cre}$ embryos at E9.5 (***a***) and E12.5 (***b–i***). The targeting strategy to generate $Emx2^{+/Cre}$ mice is given in supplemental Figure 2 (available at www.jneurosci.org as supplemental material). Whole-mount lateral (***a***), sagittal (***b***), and frontal (***c–i***) views are shown. The inset in ***b*** gives the enlarged view of the pallium in the squared area; the βGal intensity is discontinuous at a boundary (arrowheads) between the neopallium and archipallium. The squares in ***c*** indicate the sites of the enlarged views in ***d–f***, respectively: neopallium (***d***); archipallium (***e***); cortical hem, choroid plexus, and choroidal roof (***f***); thalamus (***g***); anterior pretectum (***h***); posterior pretectum (***i***). APa, Archipallium; CH, cortical hem; CP, choroid plexus; CR, choroidal roof; ET, eminentia thalami; e, eye; Fb, forebrain; GE, ganglionic eminence; HTh, hypothalamus; IM, intermediate mesoderm; Ma, mammillary region; n, nose; NPa, neopallium; Pt, pretectum; PTh, prethalamus; RMa, retromammillary region; Th, thalamus. Scale bars: ***a***, 250 μm; ***b***, ***c***, 500 μm; ***b***, inset, 125 μm; (in ***d***, ***g***) ***d–i***, 50 μm.

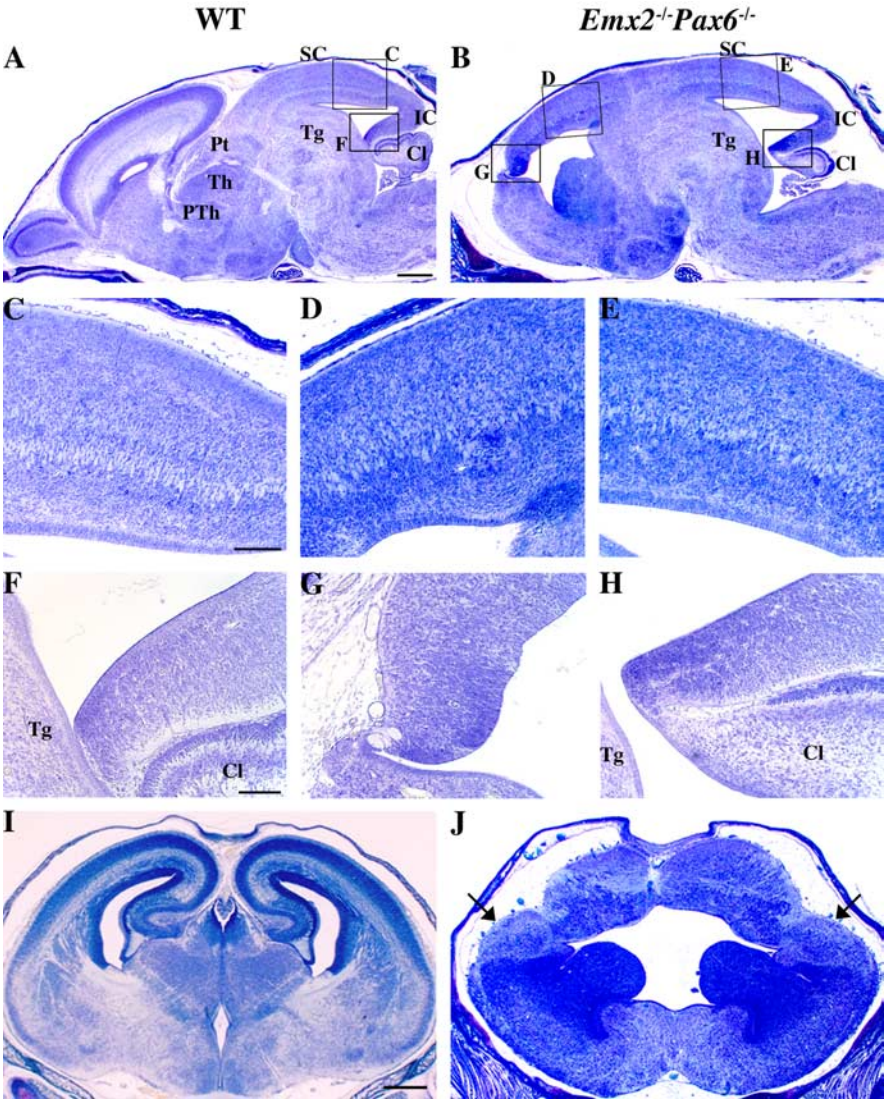

Figure 4. Tectum duplication in $Emx2^{-/-}Pax6^{-/-}$ double mutant. Parasagittal (***A–H***) and frontal (***I***, ***J***) views of E18.5 wild-type (***A***, ***C***, ***F***, ***I***) and double mutant (***B***, ***D***, ***E***, ***G***, ***H***, ***J***) brains stained with cresyl violet are shown. ***C–H***, Enlarged views of the sites indicated by the squares in ***A*** and ***B***. The arrows in ***J*** indicate the residual pallium. Cl, Cerebellum; IC, inferior colliculus; Pt, pretectum; PTh, prethalamus; SC, superior colliculus; Tg, tegmentum; Th, thalamus. Scale bars: (in ***A***) ***A***, ***B***, 500 μm; (in ***C***) ***C–E***, 125 μm; (in ***F***) ***F–H***, 100 μm; (in ***I***) ***I***, ***J***, 380 μm.

forebrain, as expected (Fig. 3*Ba*); the βGal-positive region in the forebrain was, however, more caudally expanded than the endogenous *Emx2* mRNA expression at this stage (Fig. 3*Ac*) and almost overlapped with *Pax6* mRNA expression (Fig. 3*Ag*). In the E12.5 brain, the βGal expression was evident not only in the archipallium, eminentia thalami, and prethalamus but also in the thalamus and pretectum (Fig. 3*Bb*).

Thus, the cell lineage analysis explains why the thalamus and anterior pretectum are lost in the *Emx2/Otx2* double mutant (Suda et al., 2001). The βGal staining was homogenously intense over the archipallium (Fig. 3*Bb*,*Be*), eminentia thalami (Fig. 3*Bb*), prethalamus (Fig. 3*Bb*), thalamus (Fig. 3*Bb*,*Bg*), and anterior pretectum (Fig. 3*Bb*,*Bh*); the majority of cells were βGal positive, indicating almost all of the cells in these structures once expressed *Emx2*. In contrast, in the posterior pretectum, the majority were instead βGal negative (Fig. 3*Bb*,*Bi*). Notable was the intense βGal expression in the most dorsomedial structures of the telencephalon (Fig. 3*Bb*,*Bf*). The *Emx2* mRNA expression is never found in the ventral/medial cortical hem, choroid plexus, or choroidal roof when these structures are formed (Fig. 3*Ad*) (data not shown) (Tole et al., 2000; Shinozaki et al., 2004), but the cells that constitute these structures must originate almost exclusively from the cells that once expressed *Emx2*. In the roof, the βGal staining extended from the pretectum to the telencephalic level (Fig. 3*Bf–Bi*); it was not found in the *Fgf8*-positive commissural plate (data not shown).

At E12.5, mammillary and retromammillary regions were also mostly composed of the cells that once expressed *Emx2*, and βGal-positive cells were evident in ganglionic eminences (Fig. 3*Bb*,*Bc*). In contrast, the intensity of βGal expression was apparently low in the lateral pallium (neopallium) (Fig. 3*Bb*,*Bd*). However, this could not be explained simply by the presence of βGal-negative cells; the staining intensity is influenced by cellular morphology and orientation. Of note is that the βGal staining in the pallium was not graded; the intensity was discontinuous at a boundary between the neopallium and archipallium (Fig. 3*Bb*). The lineage analysis also indicates that *Emx2*-positive cells do not contribute posteriorly to the midbrain or anteroventrally to the hypothalamus. In addition, the influx of the cells from these regions to the *Emx2*-positive region is also minimal, if any, consistent with the cell lineage analysis with vital dye (Inoue et al., 2000).

Mirror image duplication of tectum in *Emx2/Pax6* double mutant

The E18.5 $Emx2^{-/-}Pax6^{-/-}$ double mutant phenotype was unexpected and striking. The structure dorsally developing in the double mutant, in which forebrain structures develop in wild-type embryos, was obviously histologically the tectum. Furthermore, it developed in a mirror image toward the normal one. Normally, the tectum displays a distinct rostrocaudal gradient of cytoarchitectonic maturation (Fig. 4*A*); rostrally superior colliculus and caudally inferior colliculus are formed. The duplicated tectum displayed the rostrocaudally opposite cytoarchitecture (Fig. 4*B–H*). Duplication of the cerebellum did not occur. The pallium was reduced greatly; it was lost in the medial portion (Fig. 4*I*,*J*). Ganglionic eminences were present and rather hyperplastic (Fig. 4*A*,*B*,*I*,*J*); the duplication of the tegmentum was not apparent.

Normally, *En2* is expressed in the posterior midbrain at E15.5 (Fig. 5*A*) (Davis and Joyner, 1988); in the double mutant, an *En2*-positive structure was also present in the most anterior part of the "duplicated tectum" (Fig. 5*B*). *EphrinA2* is also expressed in the caudal part of the normal midbrain (Fig. 5*C*) (Flenniken et al., 1996), and the duplicated tectum expressed *EphrinA2* (Fig. 5*D*). Thus, the mirror image nature of the tectum duplication was confirmed molecularly.

At E15.5, the duplicated tectum was less pronounced than at E18.5, and at E12.5, it was even less distinct (Fig. 6*B*). The ectopic *En2* and *EphrinA2* expressions were, however, present in the E12.5 *Emx2/Pax6* double mutant (Fig. 5*F*,*H*). The *Fgf8* expression in the isthmus was unaffected. However, that in the commissural plate was caudally expanded by the $Emx2^{-/-}$ single mutation (Fig. 5*O*) (Fukuchi-Shimogori and Grove, 2003; Shinozaki et al., 2004); the expansion was more marked in the $Emx2^{-/-}Pax6^{-/-}$ double mutant (Fig. 5*N*). Consequently, the expression fused to the *Fgf8* expression in the roof of the prethalamus. At E12.5, the ectopic *En2* and *EphrinA2* expressions (Fig. 5*F*,*H*) were juxtaposed to this *Fgf8* expression (Fig. 5*J*). At E10.5, no ectopic *En2* expression was apparent (Fig. 5*L*).

Emx2 cooperates with *Pax6* in forebrain development

In E12.5 *Emx2/Pax6* double mutants, histologically an amorphous structure was present at the place where normally the thalamus/pretectum develops (Fig. 6*B*, arrow); otherwise, diencephalic structures were not apparent, and Ammon's horn also did not develop. In the $Pax6^{-/-}$ single mutant, diencephalic structures are poor but present; Ammon's horn is also apparent (supplemental Fig. 3, available at www.jneurosci.org as supplemental material) (Stoykova et al., 1996; Warren and Price, 1997). In the *Sey* diencephalon, although reduced, the *Pax6*- and *Dlx1*-positive prethalamus, *Gbx2*- and *Tcf4*-positive thalamus, and *Tcf4*- and *Ebf1*-positive pretectum are present (supplemental Fig. 3, available at www.jneurosci.org as supplemental material) (Stoykova et al., 1996). The *Ebf1*-negative and *Pax6*-/*Lim1*-positive commissure region of the pretectum scarcely exists. Thus, *Pax6* was previously concluded to function in a fine-tuning aspect of diencephalon development by regulating cell growth, but not in determination of its territory (Stoykova et al., 1996; Warren and Price, 1997). In contrast, neither the *Pax6*-/*Dlx1*-/*Lim1*-positive prethalamus (Fig. 6*D*,*F*,*N*), *Gbx2*-/*Tcf4*-positive thalamus (Fig. 6*H*,*J*), *Ebf1*-positive non-commissure region of the pretectum (Fig. 6*L*), nor *Lim1*-positive commissure region of the pretectum (Fig. 6*N*) was apparent at all in the $Emx2^{-/-}Pax6^{-/-}$ double mutant. The *Dlx1*-negative supraopto-paraventricular area was also lost (Fig. 6*F*). The amorphous structure did not express any of the diencephalic markers and was surrounded by the *Tcf4* expression (Fig. 6*J*); the structure might correspond to the most rostral midbrain structure, the griseum tectalis.

The *Shh* expression demarcates the presumptive ZLI that terminates dorsally in the *Fgf8*-positive prethalamus roof; this *Shh* expression was present in the double mutant (Fig. 6*P*), although morphologically, ZLI was never formed. Thus, the mechanism that initiates the *Shh* expression is independent of forebrain development under *Emx2* and *Pax6*. The ectopic *En2* and *EphrinA2* expressions (Fig. 5*F*,*H*) juxtaposed posteriorly to the dorsal end of this *Shh*-positive stripe, suggesting that structures rostral to the stripe are not involved in the duplication. The prethalamic region between this *Shh* stripe and the *BF1*-positive cerebrum (Fig. 6*O*, arrowhead) was absent in the *Emx2/Pax6* double mutant at E12.5

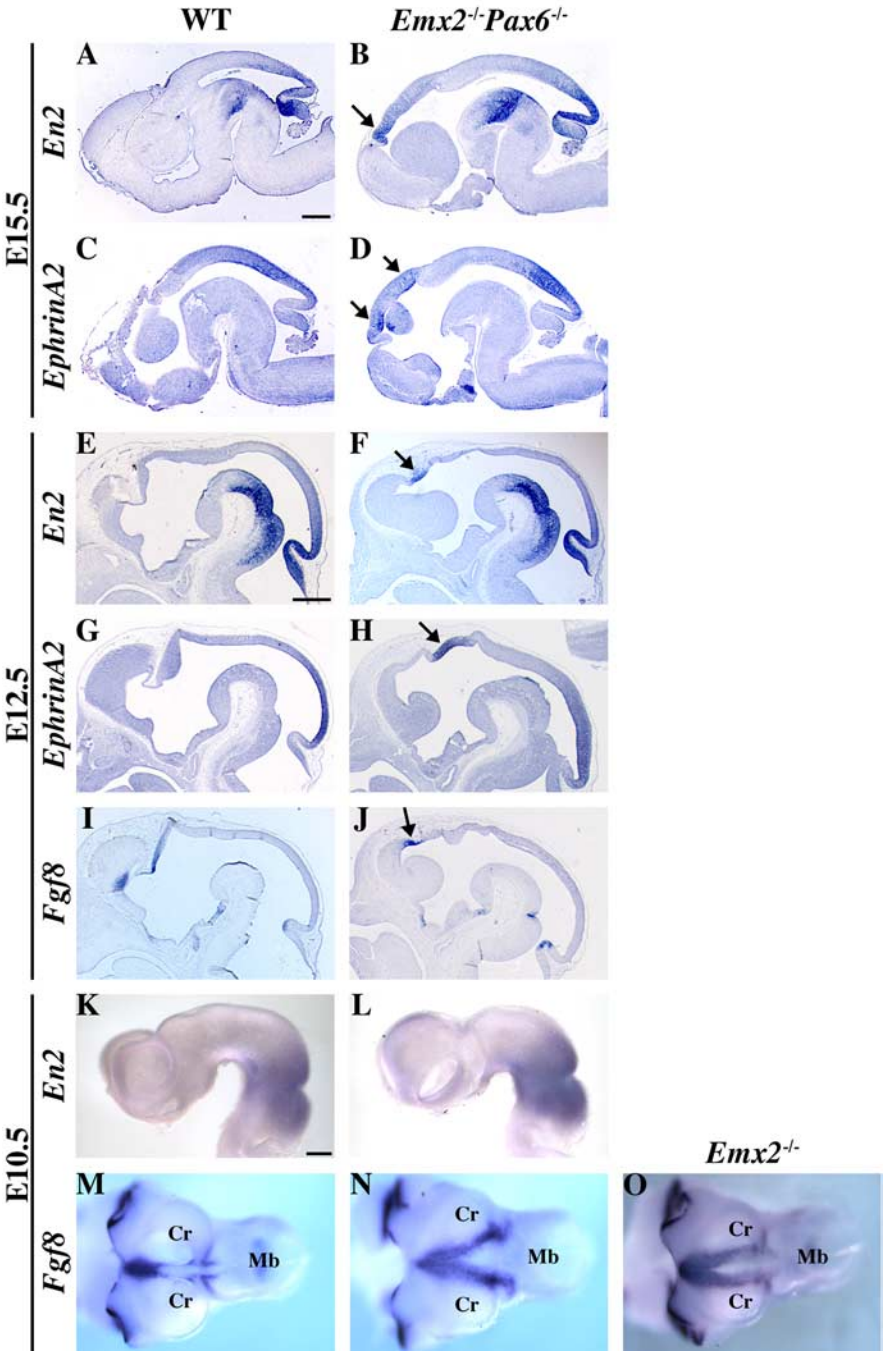

Figure 5. Marker analysis of tectum duplication in $Emx2^{-/-}Pax6^{-/-}$ double mutant. *En2* expression (***A***, ***B***, ***E***, ***F***, ***K***, ***L***), *EphrinA2* expression (***C***, ***D***, ***G***, ***H***), and *Fgf8* expression (***I***, ***J***, ***M–O***) at E15.5 (***A–D***), E12.5 (***E–J***), and E10.5 (***K–O***), respectively, in embryos of the genotype indicated at the top are shown. Mid-sagittal (***A–J***), whole-mount lateral (***K***, ***L***), and whole-mount dorsal (***M–O***) views are shown. The arrows indicate ectopic *En2* (***B***, ***F***), ectopic *EphrinA2* (***D***, ***H***), and *Fgf8* expression rostrally juxtaposed to the ectopic *En2* and *EphrinA2* expression (***J***), respectively. Cr, Cerebrum; Mb, midbrain. Scale bars: (in ***A***, ***E***) ***A–J***, 500 μm; (in ***K***) ***K–O***, 250 μm.

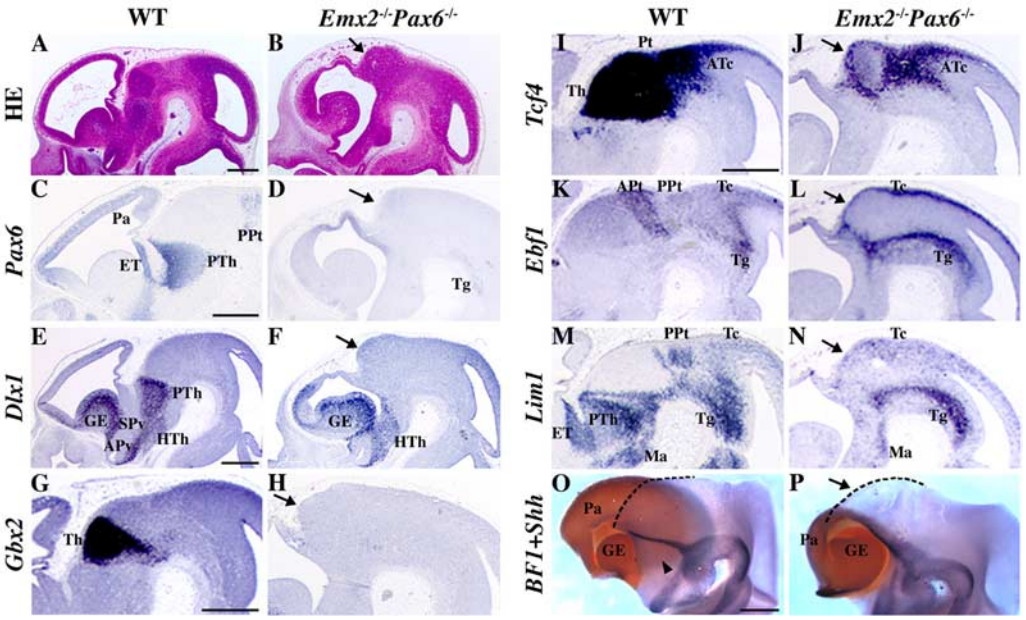

Figure 6. Marker analysis of *Emx2*$^{-/-}$*Pax6*$^{-/-}$ double mutant defects in the E12.5 diencephalon. ***A–N*** show parasagittal views. ***A***, ***B***, Histological sections stained with hematoxylin and eosin. ***C–N***, The expression of each marker is indicated to the left in embryos of the genotype indicated at the top. ***O*** and ***P*** show the medial views of hemisected brains, with the *BF1* expression in the ganglionic eminences and pallium in orange and the *Shh* expression in dark blue; dotted lines contour the dorsal limits of diencephalon. The arrows in the double mutant panels indicate the ectopic structure that does not express any of the diencephalic markers indicated. The arrowhead in ***O*** indicates the prethalamic region that is absent in the *Emx2/Pax6* double mutant (***P***). In the *Pax6* single mutant, the *Pax6*-, *Lim1*-, and *Wnt8b*-positive eminentia thalami, the *Pax6*-, *Dlx1*-, and *Lim1*-positive prethalamus, the *Gbx2*- and *Tcf4*-positive thalamus, and the *Ebf1*- and *Tcf4*-positive anterior pretectum are reduced but present; the *Pax6*- and *Lim1*-positive posterior pretectum scarcely exists (supplemental Fig. 3, available at www.jneurosci.org as supplemental material) (Stoykova et al., 1996; Warren and Price, 1997). These structures are completely lost in the *Emx2*$^{-/-}$*Pax6*$^{-/-}$ double mutant. In the double mutant, weak *Pax6* expression in the tegmentum remains (***D***), *Dlx1* expression in the ganglionic eminences and hypothalamus is retained (***F***), the *Dlx1*-negative anterior periventricular area develops, but the supraopto-paraventricular area is lost (***F***), and *Tcf4* expression is kept in the anterior tectum and surrounds the ectopic structure that does not express any diencephalic markers (***J***). Normally *Ebf1* expression is found in the anterior pretectum, tectum, and tegmentum but not in the posterior pretectum (***K***). In the double mutant, the expression in the anterior pretectum is lost and that in the tectum and tegmentum is expanded rostrally (***L***). *Lim1* expression in the mammillary region is retained, and the expression in the tectum and tegmentum is expanded rostrally (***N***). The *BF1*-positive pallium is also greatly reduced in the double mutant, but the ganglionic eminences are hyperplastic (***P***). The *Emx1*$^{-/-}$*Emx2*$^{-/-}$*Pax6*$^{-/-}$ triple mutant phenotype was the same as the double mutant one. See supplemental Figure 3 (available at www.jneurosci.org as supplemental material) for comparison of these marker phenotypes among the single, double, and triple mutants. APt, Anterior pretectum; APv, anterior periventricular area; ATc, anterior tectum; ET, eminentia thalami; GE, ganglionic eminences; HTh, hypothalamus; Ma, mammillary region; Pa, pallium; PPt, posterior pretectum; Pt, pretectum; PTh, prethalamus; SPv, supraopto-paraventricular area; Tc, tectum; Tg, tegmentum; Th, thalamus. Scale bars, 500 μm.

(Fig. 6*P*), consistent with the lack of the *Pax6-/Dlx1-/Lim1*-positive prethalamus; it is present in the *Pax6* single mutant (supplemental Fig. 3, available at www.jneurosci.org as supplemental material). The *BF1*-positive pallium was also greatly reduced in the double mutant at this stage. In these diencephalic phenotypes, the *Emx1*$^{-/-}$*Pax6*$^{-/-}$ double mutant was the same as the *Pax6*$^{-/-}$ single mutant (data not shown), and the *Emx1*$^{-/-}$*Emx2*$^{-/-}$*Pax6*$^{-/-}$ triple mutant was the same as the *Emx2*$^{-/-}$*Pax6*$^{-/-}$ double mutant (supplemental Fig. 3, available at www.jneurosci.org as supplemental material).

In the telencephalon, morphologically the choroid plexus was never apparent, and *TTR* expression was not observed in lateral ventricles of the *Emx2/Pax6* double mutant (Fig. 7*B*). The *Wnt3a*-, *Wnt5a*-, and *Wnt2b*-positive cortical hem did not exist (Fig. 7*D*) (data not shown), and the *Ephb1*- and *Prox1*-positive hippocampal field was never found (Fig. 7*F*) (data not shown). The *Wnt8b*- and *Lef1*-positive medial pallium was residual (Fig. 7*H*) (data not shown). These structures were also affected but clearly present in *Pax6*$^{-/-}$ (supplemental Fig. 4*Ab–Db*, available at www.jneurosci.org as supplemental material) (data not shown) and *Emx2*$^{-/-}$ (Yoshida et al., 1997; Shinozaki et al., 2004) single mutants.

The *Dlx1* expression extends dorsally into the neopallial region in the *Pax6*$^{-/-}$ single mutant (supplemental Fig. 4*Eb*, available at www.jneurosci.org as supplemental material) (Stoykova et al., 2000) and even more in the double mutant (Fig. 7*N*) (Muzio et al., 2002). Consequently, the *Pax6*-, *Emx1*-, and *Ngn2*-positive neopallium was greatly reduced but present at E12.5 (Fig. 7*P*,*R*,*T*); the expression of these markers overlapped ventrally with *Dlx1* expression (the dorsal limits of the *Dlx1* expression are indicated by arrows in the double mutant panels of Fig. 7). Moreover, the pallium medially expressed roof markers *Lhx5*, *Msx1*, and *Otx2* (Fig. 7*J*,*L*) (data not shown; see Discussion) (Muzio et al., 2002); apparently the *Emx2/Pax6* double mutant neopallium was incorrectly specified at E12.5. The entire pallium was, however, positive to *Lhx2* and *BF1* that are never found in the cortical hem (Fig. 7*U*,*V*) (Muzio et al., 2002) (data not shown).

The *Emx2/Pax6* double mutant roof at the telencephalic level (the medial part between the arrowheads in Fig. 7) did not express choroidal roof markers: neither *Wnt8b* nor *Lhx5* (Fig, 7*H*,*J*). Instead, the *Msx1* expression was intense (Fig. 7*L*). This was also the case in the *Emx2*$^{-/-}$*Otx2*$^{+/-}$ double mutant roof at the telencephalic level (Fig. 1). In these telencephalic phenotypes, the *Emx1*$^{-/-}$*Pax6*$^{-/-}$ double mutant was the same as the *Pax6*$^{-/-}$ single mutant, and the *Emx1*$^{-/-}$*Emx2*$^{-/-}$*Pax6*$^{-/-}$ triple mutant was the same as the *Emx2*$^{-/-}$*Pax6*$^{-/-}$ double mutant (supplemental Fig. 4, available at www.jneurosci.org as supplemental material).

Onset of *Emx2*$^{-/-}$*Pax6*$^{-/-}$ defects

At E10.5, the *En2* expression in the caudal midbrain is somewhat expanded, and the *En2*-negative rostral brain is reduced in the

Emx2$^{-/-}$*Pax6*$^{-/-}$ double mutant (Fig. 5*L*). The *Shh*-positive ZLI was also present at this stage (Fig. 8*Ab*). Of note is that at this stage a region was present between the *Shh*-positive stripe and *BF1*-positive cerebral hemispheres that corresponds to prethalamus and eminentia thalami in wild-type embryos (Fig. 8*Ab*, arrows); it was not apparent at E12.5 (Fig. 6*P*). At this stage, *BF1*-positive cerebral hemispheres were almost normal rostrally but somewhat reduced caudally. *Pax6* and *Dlx1* expressions were more properly segregated into the pallium and subpallium, respectively, at E10.5 than at E12.5 (data not shown) (Muzio et al., 2002).

At E9.5, the *Fgf8* expression in the isthmic region was normally found in the *Emx2/Pax6* double mutant (Fig. 8*Ac*,*Ad*); however, the *En2* expression was somewhat expanded, and the *En2*-negative rostral brain was slightly reduced (Fig. 8*Ae*,*Af*). In wild-type embryos, *Dmbx1* is expressed in the mesencephalon and a part of the caudal diencephalon (Fig. 8*Ag*); the *Dmbx1*-positive region was slightly enlarged, and the *BF1*- and *Dmbx1*-negative presumptive anterior diencephalon was reduced, but obviously present, in the *Emx2/Pax6* double mutant (Fig. 8*Ah*). *BF1*-positive cerebral hemispheres were somewhat reduced. E9.5 is the stage when several markers start to be expressed in the diencephalic region and subregionalization occurs at this region. One such marker is *Tcf4*, which marks the future thalamus and pretectum (Fig. 8*Ai*); the *Tcf4* expression was never observed in the *Emx2*$^{-/-}$*Pax6*$^{-/-}$ double mutant (Fig. 8*Aj*). Another marker examined is *Wnt7b* that normally marks the future archipallium, eminentia thalami, prethalamus, and a part of the thalamus (Fig. 8*Ak*); the *Wnt7b* expression was also not found in the double mutant (Fig. 8*Al*).

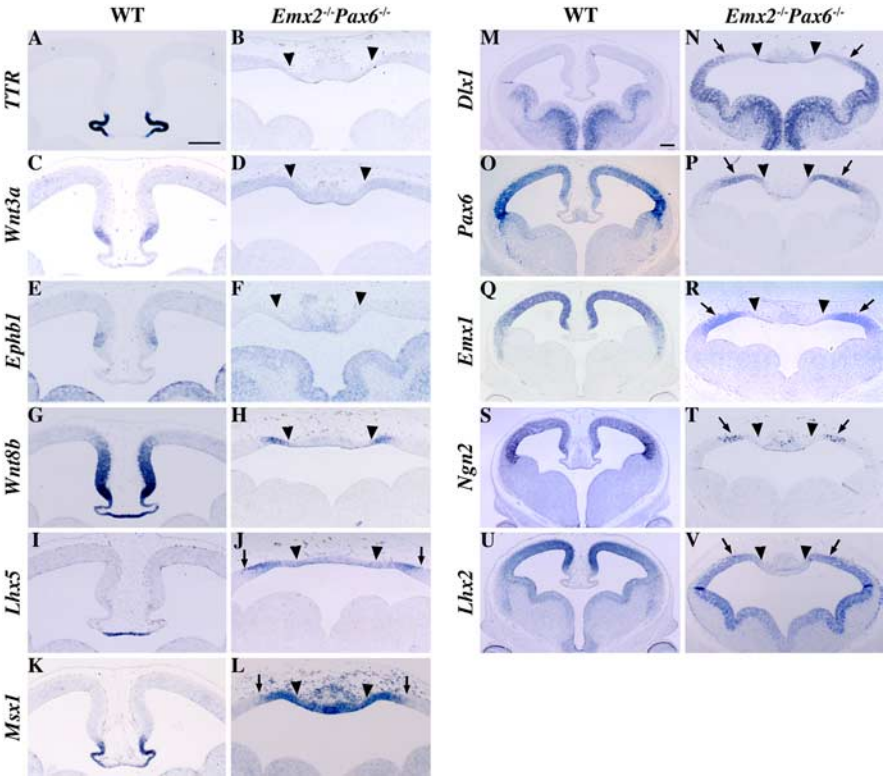

Figure 7. Marker analysis of *Emx2*$^{-/-}$*Pax6*$^{-/-}$ double mutant defects in E12.5 telencephalon. The images are frontal views of the expression of each marker indicated in embryos of the genotype shown at the top. ***A–L*** focus on the dorsomedial telencephalon, and ***M–V*** cover the entire telencephalon. In the double mutant panels, arrows indicate the dorsal limit of the *Dlx1* expression, and the arrowheads indicate the medial limits of the *Wnt8b* expression that represents the limits of the pallial regions. In the double mutant, the *TTR*-positive choroid plexus (***A***), *Wnt3a*-positive cortical hem (***C***), and *Ephb1*-positive prospective hippocampus (***E***) are absent (***B***, ***D***, ***F***). *Wnt8b* expression is residual in the medial pallium and absent in the roof (***H***). In the wild-type telencephalon, *Lhx5* expression is unique to the choroidal roof (***I***), whereas *Lhx5* is expressed ectopically in the pallium and not in the roof of the double mutant (***J***). In the double mutant, the *Msx1* expression is intense in the roof and extends laterally into the pallial region (***L***); *Dlx1* expression also extends dorsally into the pallial region (***N***). The *Pax6*-, *Emx1*-, and *Ngn2*-positive neopallium are meager in the double mutant (***P***, ***R***, ***T***). The entire pallium, however, expresses *Lhx2* that is never found in the cortical hem (***V***). The marker phenotypes of the *Emx2*$^{-/-}$*Pax6*$^{-/-}$ double mutant roof are quite similar to those of the *Emx2*$^{-/-}$*Otx2*$^{+/-}$ roof (Fig. 1). See supplemental Figure 4 (available at www.jneurosci.org as supplemental material) for comparison of these marker phenotypes among the single, double, and triple mutants. Scale bars, 240 μm.

Finally, the analysis was conducted at the 6 somite stage for the initial defects. The anterior neuroectoderm expresses *Otx2* in the region that corresponds to the future forebrain and midbrain (Fig. 8*Ba*), *Six3* in the most anterior region (Fig. 8*Bc*), and *Irx1* complementarily in the caudal aspect of the *Otx2*-positive neuroectoderm (Fig. 8*Be*). *Pax6* is expressed in the caudal forebrain primordium (Fig. 8*Bg*), and *Pax2* is expressed in the midbrain and eye primordium (Fig. 8*Bi*). No changes were apparent in any area positive to these markers in the *Emx2/Pax6* double mutant (Fig. 8*Bb*,*Bd*,*Bf*,*Bh*,*Bj*). Thus, the prospective caudal forebrain region must be almost normally present in the *Emx2*$^{-/-}$*Pax6*$^{-/-}$ double mutant at the 6 somite stage.

Discussion

Otx2/Otx1/Emx2/Pax6 and caudal forebrain

Previously, we have identified the enhancer responsible for the *Otx2* expression in the anterior neuroectoderm (AN enhancer) and reported that the *Emx2*$^{-/-}$*Otx2*$^{\Delta AN/\Delta AN}$ mutant that specifically lacks the *Otx2* expression under this enhancer exhibits the same defect in caudal forebrain development (Kurokawa et al., 2004a). The *Emx2* expression occurs around the 3 somite stage, and the AN enhancer activity is lost beyond the 6 somite stage. This indicates that the defect occurs around the 3–6 somite stage. The *Cre* knock-in mutant into the *Emx2* locus demonstrated that the *Emx2* and *Pax6* expressions initially mainly overlap and that the double mutant defects may correspond to these *Emx2* and *Pax6* expressions at the 3–6 somite stage. We propose that in the anterior neuroectoderm maintained by the *Otx2* expression under the AN enhancer (Kurokawa et al., 2004a), *Emx2* and *Pax6* establish the caudal forebrain primordium in cooperation with *Otx2* and *Otx1* at the 3–6 somite stage (Fig. 9). In this establishment, the *Emx2* and *Pax6* functions are redundant, as suggested by their single mutant phenotype; in the absence of both genes, the caudal forebrain remains unspecified even at E9.5. The caudal forebrain primordium comprises not only the future pretectum, thalamus, and prethalamus but also the eminentia thalami, archipallium, cortical hem, and choroid plexus. The choroid plexus is inherently associated with the choroidal roof; both choroid plexus cells and choroidal roof cells originated from the *Emx2*-positive region. Coincidentally, the marker analysis indicated that the choroidal roof was also lost in both the *Emx2/Otx2* and *Emx2/Pax6*

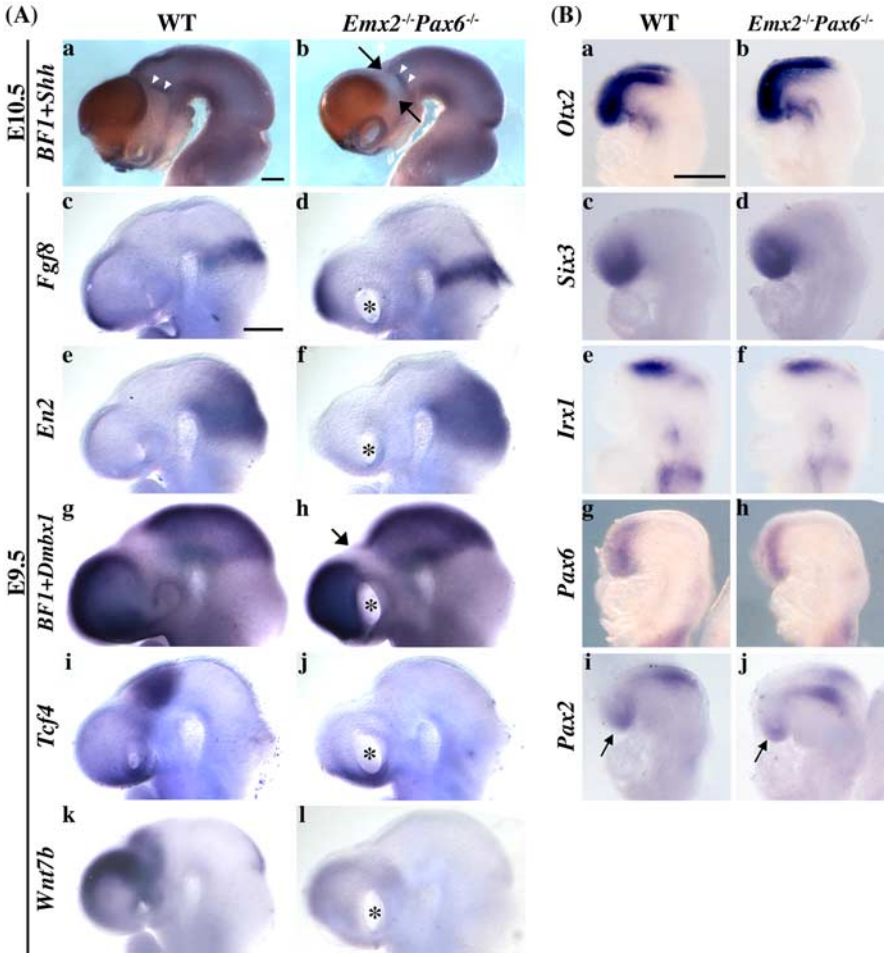

Figure 8. Onset of $Emx2^{-/-}Pax6^{-/-}$ double mutant defect. Analyses with the indicated markers at E10.5 (***Aa***, ***Ab***), E9.5 (***Ac–Al***) and the 6 somite stage (***Ba–Bj***) are shown. All images are lateral views; anterior is to the left. The arrows in ***Ab*** indicate a region between *BF1*-positive cerebral hemispheres (orange) and the *Shh*-positive stripe (dark blue); the white arrowheads in ***Aa*** and ***Ab*** indicate the stripe. The arrow in ***Ah*** indicates the *BF1*- and *Dmbx1*-negative diencephalic region. The asterisks in ***A*** indicate optic vesicles that are not converted into the optic cup by the *Pax6* mutation (Grindley et al., 1995). The arrows in ***Bi*** and ***Bj*** indicate the expression in the eyes. Scale bars, 250 μm.

double mutants. We assume that their roofs at the telencephalic level are the midbrain roofs. In contrast, not only the midbrain but also the ganglionic eminences, neopallium, and commissural plate were formed in both *Emx2/Otx2* and *Emx2/Pax6* double mutants. Defects were also not apparent in ventral structures of the forebrain.

We previously reported the loss of the archipallium, cortical hem, and choroid plexus but not the thalamic structures in the *Emx1/2* double mutant (Shinozaki et al., 2004). It occurs around E9.5 when the neural tube closes at the forebrain level and when the *Emx1* expression takes place. In contrast, the loss of the archipallium together with thalamic structures in *Emx2/Otx* and *Emx2/Pax6* double mutants is an event at the 3–6 somite stage. In the *Emx1/2* double mutant, the archipallium is transformed into the choroidal roof and the roof is expanded; we consider that this is a defect in the later dorso(roof)/ventral(alar) patterning within the p4 prosomere.

Emx2/Pax6 functions in the neopallium

Emx2 and *Pax6* are also expressed in the neopallium, and at late stages of gestation, the neopallium was abortive in both $Emx2^{-/-}Otx2^{+/-}$ and $Emx2^{-/-}Pax6^{-/-}$ double mutants (Suda et al., 2001) (Fig. 4*J*). One might propose that the telencephalic defects are graded, the dorsocaudally archipallium being more severely disrupted. However, we favor the view that the defects are discontinuous between the neopallium and archipallium. The archipallium territory was not formed at all, whereas the neopallium developed relatively normally at E10.5 in both $Emx2^{-/-}Otx2^{+/-}$ and $Emx2^{-/-}Pax6^{-/-}$ double mutants. The intensity of the *Emx2* expression was discontinuous at a boundary between the neopallium and archipallium (Fig. 3*Bb*). Of note is the fact that *cis* sequences for the *Emx2* and *Pax6* expression in the caudal forebrain primordium at the 3–6 somite stage probably do not have the activity in the neopallium (Kammandel et al., 1999; Theil et al., 2002; Kleinjan et al., 2004; our unpublished result). In addition, the enhancer of the *Emx2* expression in the neopallium does not reflect the early phase of *Emx2* expression with the onset later than the 7 somite stage. The enhancer of the *Pax6* expression in the caudal forebrain also exists separately from that in the neopallium. We assume that the *Emx2* and *Pax6* expressions in the neopallium do not function in establishing a territory; rather, these genes may have been recruited with caudorostral and mediolateral gradient of their expressions for subsequent events of neopallial development such as growth and differentiation of radial glial cells, laminar development, pallial–subpallial patterning, regulation of the influx of interneurons, and cortical arealization (Chapouton et al., 1999; Bishop et al., 2000; Mallamaci et al., 2000; Stoykova et al., 2000; Heins et al., 2002; Shinozaki et al., 2002). At the 3–6 somite stage, *Emx2* is also not expressed in the future ventral part (midline) of the caudal forebrain or prospective region of ganglionic eminences (Fig. 3*Aa*). Enhancers of the later *Emx2* expression in these regions are also different from the early enhancer (Theil et al., 2002; our unpublished result); among once *Emx2*-positive regions, $Emx2^{-/-}Otx2^{+/-}$ and $Emx2^{-/-}Pax6^{-/-}$ double mutants developed the neopallium, ganglionic eminences, and ventral diencephalon.

The *Emx2/Pax6* double mutant phenotype in the telencephalon was also analyzed by Muzio et al. (2002). We agree with their interpretation in their major issue that the neopallial territory is once formed but later respecified into a subpallial character; at E12.5, the pallium is on the way to respecification. However, Muzio et al. (2002) did not consider that the *Emx2/Pax6* double mutant defect is principally the defect in the initial brain regionalization at the 3–6 somite stage and neglected the ectopic duplication of the tectum, where normally caudal forebrain is formed. The discrepancy between our view and theirs centers on the cortical hem development. By the *Msx1*, *Otx2*, and *Id3* expression, they propose that the cortical hem fate also spread into the pallial field; *Emx2* was believed by them to cooperate with a low level of *Pax6* dorsomedially to protect the pallium against the cortical hem fate. We do not agree with this view. The cortical hem is rather reduced in the *Emx2* single mutant and lost in the *Emx1/2*

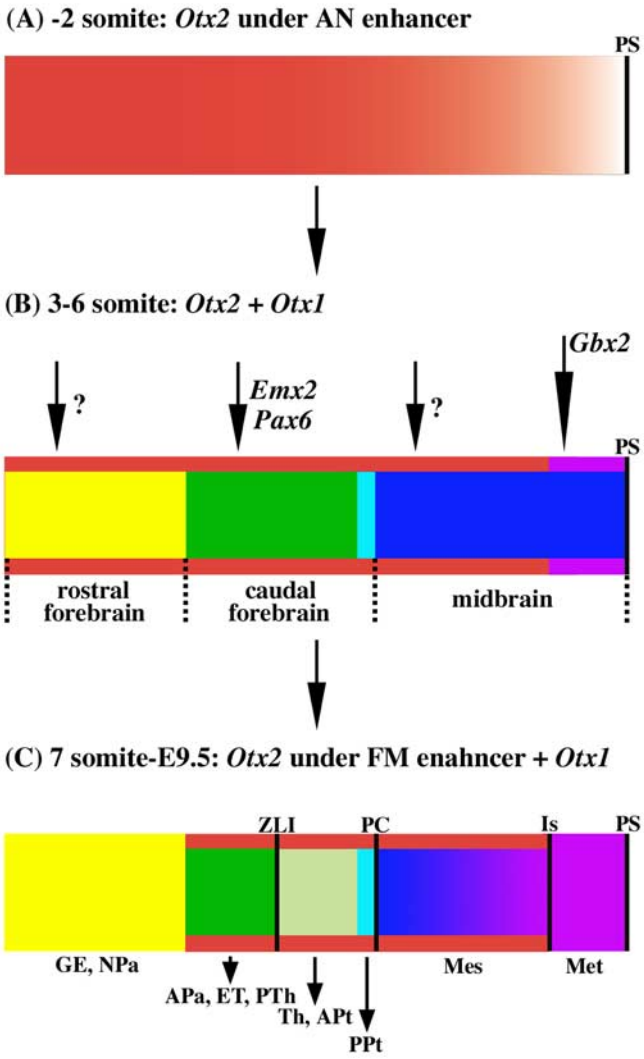

Figure 9. Schematic representation of initial regionalization of rostral brain proposed by this study. ***A***, At the 2 somite stage, the *Otx2* expression (orange) in the anterior neuroectoderm that covers the entire future forebrain and midbrain is regulated by the AN enhancer; its caudal limit is obscured in front of the preotic sulcus (PS) (Kurokawa et al., 2004a). This *Otx2* expression protects the anterior neuroectoderm against posteriorizing signals; its loss results in the transformation of the ectoderm to the *Gbx2*-positive metencephalon. ***B***, *Otx1*, *Emx2*, and *Pax6* expressions occur around the 2–4 somite stage. We propose that at the 3–6 somite stage, the anterior neuroectoderm rostral to the PS first differentiates into the three primordia: rostral forebrain, caudal forebrain, and midbrain. The caudal forebrain primordium corresponds to the *Emx2*- or *Pax6*-positive domain (dark green) at this stage; their expression mainly overlaps, but the *Pax6* expression extends caudally beyond the *Emx2* expression (light blue). To develop the caudal forebrain, *Emx2* and *Pax6* function redundantly, in cooperation with *Otx2* and *Otx1*. With the loss of both *Emx2* and *Pax6*, the caudal forebrain territory remains unspecified and secondarily transforms into the tectum, as demonstrated by this study. The loss of *Emx2* coupled with the hemizygous loss of *Otx2* results in the loss of the caudal forebrain, except the posterior (commissure region of) pretectum (PPt) (Suda et al., 2001). The *Pax6/Otx2* double mutant phenotype remains to be examined to confirm our proposal. ***C***, The *Pax6*-positive and *Emx2*-negative cells generate the posterior pretectum; the *Emx2* expression is incompatible with the development of these cells as indicated by the $Otx2^{+/Emx2}$ knock-in mutation (Suda et al., 2001). The thalamus (Th) and anterior (non-commissure region of) pretectum (APt) cells are characterized by the loss of the *Emx2* expression at E9.5 (light green); however, the continuation of the *Emx2* expression is compatible with their development as demonstrated by the $Otx2^{+/Emx2}$ mutation. In contrast, *Emx2* continues to be expressed in prethalamus (PTh), eminentia thalami (ET), and archipallium (APa) cells rostral to ZLI at E9.5 (dark green). Most dorsomedially, the caudal forebrain extends from the pretectum roof to the cortical hem, choroid plexus, and choroidal roof. The *Otx2* expression (orange) at this stage is governed by forebrain and midbrain enhancers (FM and FM2) that do not have activity in the rostral forebrain (yellow); they are active in the archipallium (Kurokawa et al., 2004b). The rostral forebrain generates the neopallium (NPa) and ganglionic eminences (GE). The *Otx2* and *Otx1* expressions at this stage protect the caudal forebrain and midbrain against posteriorizing signals. The loss of these expressions causes the transformation of the caudal forebrain and midbrain into the *Gbx2*-positive metencephalon; however, the rostral forebrain remains established even under their loss (Kurokawa et al., 2004b). *Emx1* does not play any role in this initial brain regionalization. Is, Isthmus; Mes, mesencephalon; Met, metencephalon; PC, posterior commissure.

double mutant (Yoshida et al., 1997; Shinozaki et al., 2004). The *Msx1*, *Otx2*, and *Id3* expressions are not unique to the cortical hem but also are found in the choroid plexus and roof (Fig. 7*K*) (Jen et al., 1997; Kurokawa et al., 2004a,b; Shinozaki et al., 2004). We consider that the incorrect *Msx1*, *Otx2*, and *Id3* expression in the double mutant pallium rather represents roof character and conclude that the archipallium, choroid plexus, and cortical hem are lost in the double mutant. *Lhx5* is a marker unique to the choroidal roof (Fig. 7*I*) (Shinozaki et al., 2004) and was also expressed in the double mutant pallium (Fig. 7*J*). Neither the *Wnt3a*-, *Wnt5a*-, nor *Wnt2b*-positive structure was formed, although Muzio et al. (2002) reported no changes in the expression of these markers. They also reported no change in the *Wnt8b* expression. In our double mutant, the *Wnt8b* expression was residual. The entire double mutant pallium expressed *Lhx2* and *BF1*; the cortical hem never expresses *Lhx2* or *BF1*.

Pretectum development

In the pretectum, the anterior (non-commissure) region consisted mostly of the cells that once expressed *Emx2*, but the posterior (commissure) region consisted mostly of the cells that never expressed *Emx2*. In light of the role of *Pax6* in the development of the commissure region of the pretectum (Stoykova et al., 1996; Schwarz et al., 1999) and cell lineage analysis with vital dye that indicates no cell influx from midbrain after the 5 somite stage (Inoue et al., 2000), it is most likely that the majority of cells in this region are *Pax6*-positive cells. Thus, it is probable that at the 3–6 somite stage, the *Pax6* expression caudally extends beyond the end of the *Emx2* expression, and this population of *Emx2*-negative and *Pax6*-positive cells mainly generates the commissure region of the pretectum (Fig. 9); these cells also contribute, although less extensively, to the anterior pretectum. Thus, the *Emx2* knock-in mutant into the *Otx2* locus (Suda et al., 2001) may indicate that the *Emx2* expression is incompatible with the development of these cells.

Tectum duplication in a mirror image

The presumptive caudal forebrain region developed normally at the 6 somite stage in the *Emx2/Pax6* double mutant (Fig. 8*B*); however, the region was not specified as the caudal forebrain. Instead, it transformed into an ectopic tectum in a mirror image of the original one. *Fgf8* is expressed in the roof of the prethalamus later at E9.5, and by the *Emx2* mutation, the *Fgf8* expression in the commissural plate expanded caudally. Most probably this FGF8 signaling has caused the transformation, because the region is unspecified, in the double mutant. In avian, a transplantation of FGF8-soaked beads in a diencephalic region caudal but not rostral to ZLI is known to generate an ectopic midbrain in a mirror image (Crossley et al., 1996; Martinez et al., 1999). The transplantation also duplicated the tegmentum, whereas the *Emx2/Pax6* double mutation did not. This is probably because the ventral region of the caudal forebrain is specified by a different genetic code.

In the *Emx2/Pax6* double mutant, the caudal forebrain cells rostral to ZLI were probably not involved in the formation of the ectopic tectum. The anterior end of the ectopic *En2* and *EphrinA2*

expression was juxtaposed to the caudal end of the *Fgf8* expression where the *Shh*-positive stripe ended dorsally. At E10.5, a region existed between this *Shh*-positive stripe and *BF1*-positive cerebral hemispheres, whereas this region was not identifiable by E12.5 (Figs. 6*P*, 8*Ab*). The cause of the loss of this region remains for future studies; preliminary bromodeoxyuridine uptake and terminal deoxynucleotidyl transferase-mediated biotinylated UTP nick end labeling assays suggested no marked decrease in cell proliferation or increase in cell apoptosis in this region at E10.5 (data not shown). The region might be lost by posteriorization with the anterior shift of the *Shh*-positive stripe.

References

Bishop KM, Goudreau G, O'Leary DD (2000) Regulation of area identity in the mammalian neocortex by *Emx2* and *Pax6*. Science 288:344–349.

Bosse A, Zulch A, Becker N, Torres M, Gomez-Skarmeta JL, Modolell J, Gruss P (1997) Identification of the vertebrate Iroquois homeobox gene family with overlapping expression during early development of the nervous system. Mech Dev 69:169–181.

Bulfone P, di Blas E, Gulisano MH, Frohman MA, Martin GR, Rubenstein JLR (1993) Spatially restricted expression of *Dlx-1*, Dlx-2 (*Tes-1*), *Gbx-2*, and *Wnt-3* in the embryonic day 12.5 mouse forebrain defines potential transverse and longitudinal segmental boundaries. J Neurosci 13:3155–3172.

Chapouton P, Gärtner A, Götz M (1999) The role of *Pax6* in restricting cell migration between developing cortex and basal ganglia. Development 126:5569–5579.

Crossley PH, Martinez S, Martin GR (1996) Midbrain development induced by FGF8 in the chick embryo. Nature 380:66–68.

Davis CA, Joyner AL (1988) Expression patterns of the homeo box-containing genes *En-1* and *En-2* and the proto-oncogene *int-1* diverge during mouse development. Genes Dev 2:1736–1744.

Dressler GR, Deutsch U, Chowdhury K, Nornes HO, Gruss P (1990) *Pax2*, a new paired-box-containing gene and its expression in the developing excretory system. Development 109:787–795.

Echelard Y, Epstein DJ, St-Jacques B, Shen L, Mohler J, McMahon JA, McMahon AP (1993) Sonic hedgehog, a member of a family of putative signaling molecules, is implicated in the regulation of CNS polarity. Cell 75:1417–1430.

Flenniken AM, Gale NW, Yancopoulos GD, Wilkinson DG (1996) Distinct and overlapping expression patterns of ligands for Eph related receptor tyrosine kinases during mouse embryogenesis. Dev Biol 179:382–401.

Fujii T, Pichel JG, Taira M, Toyama R, Dawid IB (1994) Expression patterns of the murine LIM class homeobox gene *lim1* in the developing brain and excretory system. Dev Dyn 199:73–83.

Fukuchi-Shimogori T, Grove EA (2003) Emx2 patterns the neocortex by regulating FGF positional signaling. Nat Neurosci 6:825–831.

Garel S, Marin F, Mattei MG, Vesque C, Vincent A, Charnay P (1997) Family of *Ebf/Olf-1*-related genes potentially involved in neuronal differentiation and regional specification in the central nervous system. Dev Dyn 210:191–205.

Grindley JC, Davidson DR, Hill RE (1995) The role of *Pax-6* in eye and nasal development. Development 121:1433–1442.

Grove EA, Tole S, Limon J, Yip L, Ragsdale CW (1998) The hem of the embryonic cerebral cortex is defined by the expression of multiple *Wnt* genes and is compromised in *Gli3*-deficient mice. Development 125:2315–2325.

Heins N, Malatesta P, Cecconi F, Nakafuku M, Tucker KL, Hack MA, Chapouton P, Barde YA, Götz M (2002) Glial cells generate neurons: the role of the transcription factor Pax6. Nat Neurosci 5:308–315.

Hill RE, Jones PF, Rees AR, Sime CM, Justice MJ, Copeland NG, Jenkins NA, Graham E, Davidson DR (1989) A new family of mouse homeo box-containing genes: molecular structure, chromosomal location, and developmental expression of Hox-7.1. Genes Dev 3:26–37.

Hill RE, Favor J, Hogan BL, Ton CC, Saunders GF, Hanson IM, Prosser J, Jordan T, Hastie ND, van Heyningen V (1991) Mouse *Small eye* results from mutations in a paired-like homeobox-containing gene. Nature 354:522–525.

Inoue T, Nakamura S, Osumi N (2000) Fate mapping of the mouse prosencephalic neural plate. Dev Biol 15:373–383.

Jen Y, Manova K, Benezra R (1997) Each member of the Id gene family exhibits a unique expression pattern in mouse gastrulation and neurogenesis. Dev Dyn 208:92–106.

Kammandel B, Chowdhury K, Stoykova A, Aparicio S, Brenner S, Gruss P (1999) Distinct *cis*-essential modules direct the time-space pattern of the *Pax6* gene activity. Dev Biol 205:79–97.

Kleinjan DA, Seawright A, Childs AJ, van Heyningen V (2004) Conserved elements in *Pax6* intron 7 involved in (auto)regulation and alternative transcription. Dev Biol 265:462–477.

Kobayashi D, Kobayashi M, Matsumoto K, Ogura T, Nakafuku M, Shimamura K (2002) Early subdivisions in the neural plate define distinct competence for inductive signals. Development 129:83–93.

Korinek V, Barker N, Willert K, Molenar M, Roose J, Wagenaar G, Markman M, Lamers W, Drestree O, Clevers H (1998) Two members of the Tcf family implicated in Wnt/β-catenin signaling during embryogenesis in the mouse. Mol Cell Biol 18:1248–1256.

Kurokawa D, Takasaki N, Kiyonari H, Nakayama R, Kimura-Yoshida C, Matsuo I, Aizawa S (2004a) Regulation of *Otx2* expression and its functions in mouse epiblasts and anterior neuroectoderm. Development 131:3307–3317.

Kurokawa D, Kiyonari H, Nakayama R, Kimura-Yoshida C, Matsuo I, Aizawa S (2004b) Regulation of *Otx2* expression and its functions in mouse forebrain and midbrain. Development 131:3319–3331.

Lagutin OV, Zhu CC, Kobayashi D, Topczewski J, Shimamura K, Puelles L, Russell HR, McKinnon PJ, Solnica-Krezel L, Oliver G (2003) Six3 repression of Wnt signaling in the anterior neuroectoderm is essential for vertebrate forebrain development. Genes Dev 17:368–379.

Larsen CW, Zeltser LM, Lumsden A (2001) Boundary formation and compartition in the avian diencephalon. J Neurosci 21:4699–4711.

Liu A, Joyner AL (2001) EN and GBX2 play essential roles downstream of FGF8 in patterning the mouse mid/hindbrain region. Development 128:181–191.

Mallamaci A, Muzio L, Chan CH, Parnavelas J, Boncinelli E (2000) Area identity shifts in the early cerebral cortex of *Emx2*$^{-/-}$ mutant mice. Nat Neurosci 3:679–686.

Martinez S, Crossley PH, Cobos I, Rubenstein JL, Martin GR (1999) FGF8 induces formation of an ectopic isthmic organizer and isthmocerebellar development via a repressive effect on Otx2 expression. Development 126:1189–2000.

Martinez-Barbera JP, Rodriguez TA, Beddington RS (2000) The homeobox gene *Hesx1* is required in the anterior neural ectoderm for normal forebrain formation. Dev Biol 223:422–430.

Matsuo I, Kuratani S, Kimura C, Takeda N, Aizawa S (1995) Mouse *Otx2* functions in the formation and patterning of rostral head. Genes Dev 9:2646–2658.

Miyamoto T, Kawahara A, Teufel A, Mukhopadhyay M, Zhao Y, Dawid IB, Westphal H (2002) *Mbx*, a novel mouse homeobox gene. Dev Genes Evol 212:104–106.

Muzio L, DiBenedetto B, Stoykova A, Boncinelli E, Gruss P, Mallamaci A (2002) Conservation of cerebral cortex into basal ganglia in *Emx2*$^{-/-}$ *Pax6*$^{Sey/Sey}$ double-mutant mice. Nat Neurosci 5:737–745.

Oliver G, Mailhos A, Wehr R, Copeland GN, Jenkins AN, Gruss P (1995) *Six3*, a murine homologue of the *sine oculis* gene, demarcates the most anterior border of the developing neural plate and is expressed during eye development. Development 121:4045–4055.

Parr BP, Shea MJ, Vassileva G, McMahon AP (1993) Mouse *Wnt* genes exhibit discrete domains of expression in the early embryonic CNS and limb buds. Development 119:247–261.

Porter FD, Drago J, Xu Y, Cheema SS, Wassif C, Huang SP, Lee E, Grinberg A, Massalas JS, Bodine D, Alt F, Westphal H (1997) *Lhx2*, a LIM homeobox gene, is required for eye, forebrain, and definitive erythrocyte development. Development 124:2935–2944.

Puelles L, Rubenstein JL (1993) Expression patterns of homeobox and other putative regulatory genes in the embryonic mouse forebrain suggest a neuromeric organization. Trends Neurosci 16:472–479.

Puelles L, Rubenstein JL (2003) Forebrain gene expression domains and the evolving prosomeric model. Trends Neurosci 26:469–476.

Roelink H, Nusse R (1991) Expression of two members of the *Wnt* family during mouse development-restricted temporal and spatial patterns in the developing neural tube. Genes Dev 5:381–388.

Schwarz M, Alovarez-Bolado G, Dressler G, Urbanek P, Busslinger M, Gruss

P (1999) Pax2/5 and Pax6 subdivide the early neural tube into three domains. Mech Dev 82:29–39.

Sheng HZ, Bertuzzi S, Chiang C, Shawlot W, Taira M, Dawid I, Westphal H (1997) Expression of murine *Lhx5* suggests a role in specifying the forebrain. Dev Dyn 208:266–277.

Shinozaki K, Miyagi T, Yoshida M, Miyata T, Ogawa M, Aizawa S, Suda Y (2002) Absence of Cajal-Retzius cells and subplate neurons associated with defects of tangential cell migration from ganglionic eminence in E*mx1/2* double mutant cerebral cortex. Development 129:3479–3492.

Shinozaki K, Yoshida M, Nakamura M, Aizawa S, Suda Y (2004) *Emx1* and *Emx2* cooperate in initial phase of archipallium development. Mech Dev 121:475–489.

Simeone A, Gulisano M, Acampora D, Stornaiuolo A, Rambaldi M, Boncinelli E (1992) Two vertebrate homeobox genes related to the *Drosophila empty spiracles* gene are expressed in the embryonic cerebral cortex. EMBO J 11:2541–2550.

Sommer L, Ma Q, Anderson DJ (1996) *neurogenins*, novel family of atonal-related bHLH transcription factors, are putative mammalian neuronal determination genes that reveal progenitor cell heterogeneity in the developing CNS and PNS. Mol Cell Neurol 8:221–241.

Soriano P (1999) Generalized *lacZ* expression with the ROSA26 Cre reporter strain. Nat Genet 21:70–71.

Stoykova A, Fritsch R, Walther C, Gruss P (1996) Forebrain patterning defects in *Small eye* mutant mice. Development 122:3453–3465.

Stoykova A, Treichel D, Hallonet M, Gruss P (2000) *Pax6* modulates the dorsoventral patterning of the mammalian telencephalon. J Neurosci 20:8042–8050.

Suda Y, Matsuo I, Aizawa S (1997) Cooperation between *Otx1* and *Otx2* genes in developmental patterning of rostral brain. Mech Dev 69:125–141.

Suda Y, Hossain ZM, Kobayashi C, Hatano O, Yoshida M, Matsuo I, Aizawa S (2001) *Emx2* directs the development of diencephalon in cooperation with *Otx2*. Development 128:2433–2450.

Tao W, Lai E (1992) Telencephalon-restricted expression of *BF-1*, a new member of the *HNF-3/fork head* gene family, in the developing rat brain. Neuron 8:957–966.

Theil T, Aydin S, Koch S, Grotewold L, Rüther U (2002) Wnt and Bmp signaling cooperatively regulate graded *Emx2* expression in the dorsal telencephalon. Development 129:3045–3054.

Tole S, Goudreau G, Assimacopoulos S, Grove EA (2000) *Emx2* is required for growth of the hippocampus but not for hippocampal field specification. J Neurosci 20:2618–2625.

Wakasugi S, Maeda S, Shimada K, Nakashima H, Migita S (1985) Structural comparison between mouse and human prealbumin. J Biochem 98:1707–1714.

Warren N, Price DJ (1997) Roles of *Pax-6* in murine diencephalic development. Development 124:1573–1582.

Wilkinson DG (1993) In situ hybridization. In: Essential developmental biology: a practical approach (Stern CD, Holland PWH, eds), pp 257–274. Oxford: IRL.

Yagi T, Tokunaga T, Furuta Y, Nada S, Yoshida M, Tsukada T, Saga Y, Takeda N, Ikawa Y, Aizawa S (1993a) A novel ES cell line, TT2, with high germline-differentiating potency. Anal Biochem 214:70–76.

Yagi T, Nada S, Watanabe N, Tamemoto H, Kohmura N, Ikawa Y, Aizawa S (1993b) A novel negative selection for homologous recombinants using diphtheria toxin A fragment gene. Anal Biochem 214:77–86.

Yamamoto M, Meno C, Sakai Y, Shiratori H, Mochida K, Ikawa Y, Saijoh Y, Hamada H (2001) The transcription factor FoxH1 (FAST) mediates Nodal signaling during anterior-posterior patterning and node formation in the mouse. Genes Dev 15:1242–1256.

Yoshida M, Suda Y, Matsuo I, Miyamoto N, Takeda N, Kuratani S, Aizawa S (1997) *Emx1* and *Emx2* functions in development of dorsal telencephalon. Development 124:101–111.